Modelling the Rongorongo tablets: A new transcription of the Échancrée tablet and the foundation for decipherment attempts

Lorenzo Lastilla
Department of Computer, Control and Management Engineering Antonio Ruberti (DIAG), Sapienza University of Rome, Italy and

Roberta Ravanelli, Miguel Valério, and Silvia Ferrara
Department of Classical Philology and Italian Studies (FICLIT), Alma Mater Studiorum—University of Bologna, Italy

Abstract

The Rongorongo is a system of writing, still undeciphered, from Easter Island in the Pacific. It consists of a corpus of twenty-six inscriptions, scattered around the world. This article presents the state-of-the art in the study of one of these inscriptions, Text D or the 'Échancrée' tablet housed in a museum in Rome, Italy. Through an integrated methodology based on photogrammetry and high-precision structured light scanning, a 3D model of the inscriptions is made available through a public 3D Viewer for the first time. The technique made use of the benefits of both methods of image acquisition: a very accurate, precise, high resolution, and metric reconstruction of the tablet geometry gained through the scanning process, and a high-quality texture achieved through photogrammetry. In addition, we present a new analysis of the text, through a close palaeographic examination of its signs, and corrections of previous hand drawings and transcriptions. The ultimate aim is to reach unbiased 'readings' of the signs through an integrated synergy of traditional palaeographic analysis and an advanced 3D model. These, applied to all the inscriptions, constitute the necessary stepping-stones for any decipherment attempt.

Correspondence: Silvia Ferrara, Department of Classical Philology and Italian Studies (FICLIT), Alma Mater Studiorum—University of Bologna, Via Zamboni, 33, 40126 Bologna BO, Italy. E-mail: s.ferrara@unibo.it

1 The Rongorongo Inscriptions

The Rongorongo script of Easter Island or Rapa Nui was first discovered by outsiders in 1864 and has survived on about twenty-six inscribed objects (labelled A–Z), which were collected in a short span of time after their discovery (Barthel, 1958, p. 2; Fischer, 1997). These inscriptions, some of which are very long, contain a system of notation with an uncertain number of individual signs, often called 'glyphs'. The reference catalogue to this day is Barthel (1958), which lists 599 sign shapes. However, this repertoire includes sign variants ('allographs') and some compound signs ('ligatures'), but not all. Thus, it

doi:10.1093/llc/fqab045

cannot be considered definitive (Pozdniakov, 1996; Pozdniakov and Pozdniakov, 2007).

There is ongoing debate surrounding the origins of the script, and any potential influence from the outside on its shapes and internal structure (logographic, syllabic, other) remains to be proved. The shapes of the signs do not resemble any known script, and thus they appear to have been invented from zero. Whatever the status of its creation, Rongorongo shares a characteristic common to all image-based invented scripts, namely that its signs are highly iconic: their shapes depict real or fictional things, including human figurations and body parts, animals, plants, tools and other human-made objects, heavenly bodies, etc. The use of these numerous signs in complex ligatures and long, linear sequences, typically in reverse boustrophedon, strongly suggests that we are dealing with proper language notation. At least in one case (Text I or Santiago Staff), sign sequences are interspersed with possible 'sentence' or 'paragraph' dividers. Yet despite promising efforts, Rongorongo remains undeciphered and it has not yet been demonstrated beyond doubt that it constitutes a phonetic script.

Both Barthel (1958) and Fischer (1997) published catalogues of the inscriptions with normalized drawings of the texts, which are now the main references for researchers. However, they do not always agree, and vary a great deal in terms of accuracy (Horley and Pozdniakov, 2018, p. 92). In recent years, Horley (2009, 2013) has extensively studied the palaeography of Rongorongo inscriptions and is currently producing new line drawings. This latest research is revealing hitherto unnoticed cases of 'scribal' corrections (Horley, 2009, 2011; Horley and Pozdniakov, 2018, p. 92–93), which reinforce the notion that Rongorongo constitutes true writing. While this new wave of scholarship contributes to substantial progress, the palaeography and sign repertoire of Rongorongo still require further detailed examination. The number of inscriptions is limited, and even so they are scattered in eleven collections and museums across several European countries, Chile, and the USA, including Hawaii.[1] Thus, direct access to the objects and their examination remain challenging tasks.

The beginning of scholarly work on the script is associated with one event in 1869, when a German priest and a native of Rapa Nui brought a large ball of human hair as a gift to Étienne 'Tepano' Jaussen, the Bishop of Tahiti (Fischer, 1997, p. 21–24; Horley and Pozdniakov, 2018, p. 82, Fig. 2). The hair formed a rope of 20 m, which proved to be wrapped around a 'piece of board'. This wooden board, nowadays known as Échancrée (French for 'notched') or Text D,[2] was inscribed with Rongorongo signs. The inscription on it is relatively short, and the board somewhat damaged, but it sparked Jaussen's interest in the script and launched a new field of research.

This article focuses specifically on this tablet. We present an advanced 3D model of the object geared towards reassessing the extant handmade line-drawings and its palaeographic characteristics, and offering a new transcription of the texts, even in its damaged areas. These endeavours represent the founding base for any future decipherment of the Rongorongo inscriptions. Indeed, 3D digitization processes are ongoing (on method and results see Lastilla et al., 2019a, b; Esen-Baur and Santos, 2019, report their results with Tablet O in Berlin). Modelling in three dimensions tied with a palaeographic analysis is part of an ongoing programme of our EU-funded ERC INSCRIBE ('Invention of Scripts and their Beginnings', https://site.unibo.it/inscribe/en/about-1) project, based at the University of Bologna, Italy. One of the goals of the project is to produce a state-of-the-art, digital corpus that will go beyond traditional standards. This is geared towards a more in-depth analysis of the still undeciphered ancient scripts in the world, using a synergy of traditional palaeographic methods of analysis and advanced technologies in digital humanities and computer science.

2 The Échancrée Tablet: Physical and Epigraphic Description

After its discovery, the Échancrée tablet became part of the collection of the Congregation of the Sacred Hearts of Jesus and Mary, in Rome, where it is now housed. Until recently, it was on loan at the Musée de Tahiti et des Îles, at Punaauia (Tahiti). During that time, it was one of the few Rongorongo inscriptions still located in Polynesia (alongside inscriptions T, U,

V, and W, housed at the Bernice Bishop Museum, in Honolulu, Hawaii).

The tablet has already been discussed and illustrated (see Fischer, 1997, p. 421, for a relatively recent list of works). It is relatively small as it measures 23.9 × 12.3 × 2.4 cm (Barthel, 1958, p. 19 and Fischer, 1997, p. 421 report 30 × 15 cm).[3] In relation to its condition, Fisher states: 'Post-carving damage includes numerous scratches, some smaller gouges, a deep gash (perhaps to accommodate the human hair that was once wrapped around it), and notches top and bottom (perhaps for fishing lines, indicating an earlier, post-1864 use)'.

Unlike some of the other Rongorongo tablets, the surfaces of the Échancrée are flat rather than fluted. Fluting consisted in creating very shallow grooves, a few tenths of a millimeter deep, on the surface of a board. This created a ruling that accommodated the signs in a linear fashion and protected them from wearing off (Fischer, 1997, p. 388; Horley, 2009).

Orliac (2007, p. 9, 2010, p. 132–133, Table 8) has confirmed the identification of the wood of the Échancrée as *Podocarpus sp.* (cf. *Latifolia*), a tree commonly known as real yellowwood. This is the same wood she identified in three other inscribed Rongorongo objects: Texts N ('Small Vienna'), P ('Large St. Petersburg'), and S ('Large Washington'). Because real yellowwood never grew on Rapa Nui (it is native to southern Africa), Orliac (2010, p. 132) even suggested that the four boards 'were carved from the same piece of foreign wood' in 'approximately the same period'. The dimensions and shape of N, P, and S lend some support to this idea.[4] A detailed analysis of the Échancrée can therefore establish whether the possible common origin of its medium is paralleled by shared palaeographic or textual features with these three inscriptions (see Section 4).

The text of the Échancrée was written from left-to-right in reverse boustrophedon, like other tablets, but the precise reading direction of its two sides (henceforth Da and Db) is unclear. There are four theoretical possibilities (Pozdniakov, 1996, p. 298):

(1) Da1–Da8 > Db1–Db6.
(2) Da1–Da8 > Db6–Db1.
(3) Da8–Da1 > Db6–Db1.
(4) Da8–Da1 > Db1–Db6.

The Échancrée preserves visible traces or the totality of at least 212 graphic elements, composed of self-standing or composite sign shapes (see Section 4). Barthel (1958, p. 20) and Fischer (1997, p. 421) reported ca. 270 following less conservative criteria of individualization. The glyphs on side A (ca. 1.3–1.6 cm) are slightly smaller in size than those on side B (ca. 1.5–2 cm). This is possibly due to more space being available on side B, which has fewer lines of inscription, as preserved.

3 New Technologies

3.1 Introduction to the 3D techniques

The state-of-the-art in the acquisition of 3D models uses several established techniques such as photogrammetry or laser scanning (Remondino et al., 2005). However, these techniques must satisfy stricter requirements than normal archaeological objects, in terms of resolution, precision, and accuracy to reconstruct inscriptions (Spring and Caradoc, 2014; D'Aranno et al., 2016; Carrero-Pazos and Espinosa-Espinosa, 2018; Francolini et al., 2018; Valente and Barazzetti, 2020). Crucially, the glyphs on the Échancrée tablet are not deeply incised if we compare their depth, which amounts to ∼0.2 mm, with the thickness of the object, which averages 24 mm. Indeed, high-resolution and precise 3D models of inscriptions of such characteristics would allow for an easier and unbiased analysis and interpretation (Francolini et al., 2018; Lastilla et al., 2019a). The other main challenges to the 3D reconstruction of the Rongorongo text D are the tablet's wood, which is highly reflective and dark, and the tablet's edges, which must be acquired with particular care.

To produce a 3D model of the Rongorongo text D, we followed a procedure that integrated photogrammetric and structured light scanning (SLS) outputs (Lastilla et al., 2019a). This made use of the benefits of both techniques: a very accurate, precise, high resolution and metric reconstruction of the tablet geometry gained through the scanning process, and a high-quality texture achieved through photogrammetry.

3.2 Scanner

As to the scanning stage of our workflow, the ScanRider 1.2 model by VGER was used due to its

high performances in terms of nominal precision, accuracy, and resolution, necessary to reconstruct the smallest details of the tablet (Affatato et al., 2017; Lastilla et al., 2019a, b). The ScanRider 1.2 scanner implements the structured light (SL) technique through a Digital Light Processing projector and an industrial black and white camera, but it is not equipped with a color camera, thus it cannot provide texture to the 3D models.

The scanning process follows an initial stage of calibration to estimate the camera and projector parameters and to define a 3D reference frame. The scanner is capable of acquiring different sides of the same object separately and merging them at a later stage, by means of its software SpaceRider.

ScanRider 1.2 can adopt three different scanning volumes, according to the object size and complexity: the smaller the volume, the more precise and accurate the model (see Table 1 for more details).

To find a compromise between overall accuracy and to avoid acquiring an excessive amount of data, we used the intermediate scanning volume (nominal standard deviation $\leq$ 0.07 mm). The object was acquired in two sections with 330 scans. In this way, we optimized the optical parameters of the scanner, such as the exposure of the camera and the depth of field of the projector. Within the SpaceRider software, the raw scans were firstly co-registered with an alignment error of 0.05 mm, and then cleaned, fused, and smoothed, producing the high-resolution 3D model of the Échancrée tablet, featuring more than 9 million vertices and 19 million faces.

3.3 Photogrammetry

The photogrammetric 3D model was captured with the back dual wide camera of the iPad Pro 2020 12.9″ (Table 2), which allowed us to acquire images easily.

Table 2. iPad Pro 2020 12.9″ back dual wide camera specifications

Resolution (pixel)	Focal length (mm)	Aperture (−)
4,032 × 3,024	3	f/1.8

Overall, 462 images were captured in two separate sessions, where the tablet was positioned, respectively, with one of the two flat sides facing upwards (Fig. 3). We relied on natural sunlight and a white neutral background for creating a diffuse light effect, able to reduce reflections and shadows to a minimum (Fig. 3).

The images were captured moving the camera around the subject and framing the scene from different, but partially overlapping, views (Fig. 4). Particular attention was paid to collecting a high number of images of the signs on line Da8, which Barthel (1958, p. 53), unlike Fischer (1997), did not transcribe. The same applied to the edges of the tablet needed to align the two faces of the object in the 3D model. Few scale bars were added to the scene for the rough scaling of the orthomosaic (see Section 3.7). No scale bar was employed during the processing of the photogrammetric 3D model, since this 3D model was used only to provide the texture to the final overall 3D model.

We used the Agisoft Metashape software for photogrammetry (Agisoft Metashape, 2020a), formerly known as Agisoft Photoscan, based on the Structure from Motion technique. First, the two subsets of the images, corresponding to the 'top' and 'bottom' views of the tablet (Fig. 3), were separately aligned and processed at a low resolution, to produce the masks automatically for the final alignment stage. In this way, every image could be masked based on the shape of the tablet (Fig. 5) and it was possible to process all of

Table 1. Scanning volume specifications of the VGER ScanRider 1.2 scanner

	Volume 1	Volume 2	Volume 3
Volume maximum size (mm)	66 × 50 × 50	133 × 100 × 100	300 × 225 × 225
Object maximum size (mm)	66	133	150
Standard resolution (mm)	≤0.05	≤0.1	≤0.23
Precision (mm)	up to 0.03	up to 0.07	up to 0.15
Mean error (mm)	up to 0.01	up to 0.03	up to 0.05
Working distance (mm)	120	200	520

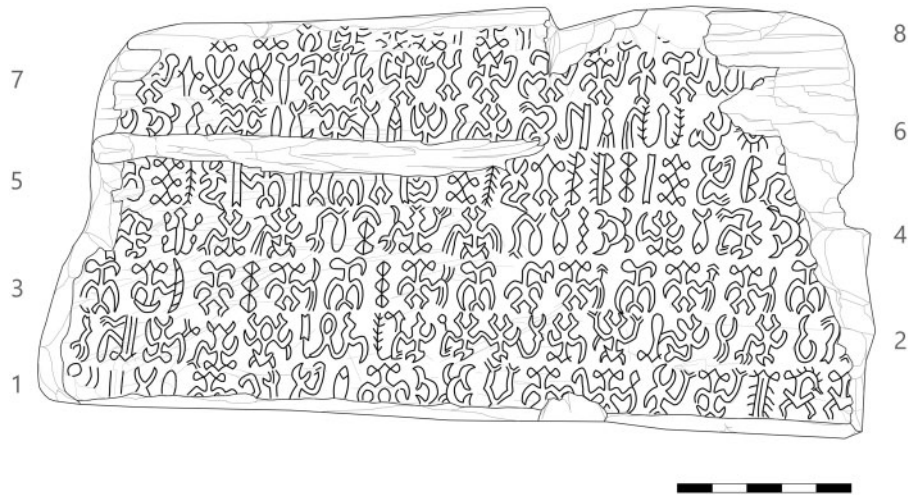

Fig. 1 Drawing of side A of the Échancrée tablet, made after the 3D model. The line numbering follows Barthel (1958)

Fig. 2 Drawing of side B of the Échancrée tablet, made after the 3D model. The line numbering follows Barthel (1958)

them together, in a single batch, relying on the tie points—identified by the matching algorithms implemented in Agisoft Metashape—placed on the edges of the object for the alignment of the two faces. This allows to obtain better quality in terms of accuracy of the 3D model, if compared with the alternative chunking method (separate processing of the subsets) (Agisoft Metashape, 2020b) which often requires markers to be added manually.

The final alignment of the 462 images was performed using the highest accuracy option and restricting the search for key points to the unmasked pixels (Fig. 5). The alignment was then refined by automatically removing the uncertain tie points and optimizing the estimation of the camera model parameters on the remaining tie points. At the end of the alignment stage, a sparse point cloud of about 30,000 points was produced with a mean root mean square (RMS) reprojection error of 0.66 pixels. Thereafter, the sparse point cloud was densified using the medium quality option, since this resolution produced the best quality in terms of texture, and, at the

Fig. 3 Photogrammetric capturing scenario: example of images of side A (left) and side B (right) captured in the two separate sessions

Fig. 4 Photogrammetric capturing scenario: in red the top views, in blue the bottom views

same time, did not generate an excessive amount of data. Starting from the dense cloud, the mesh and the texture were finally generated, creating the photogrammetric 3D model of the Échancrée tablet, featuring more than 200,000 vertices and texture coordinates (i.e. the vertex coordinates expressed in the texture—or UV—2D space, based on the UV mapping defined for the 3D model), and about 400,000 faces.

Fig. 5 Mask automatically generated for the image shown in Fig. 3 (right) and corresponding tie points automatically identified by the matching algorithms implemented in Agisoft Metashape

3.4 Texture Baking

The SL scanner provided us with a very accurate, precise, high resolution, and scaled but untextured 3D model. The photogrammetric model is characterized instead by high-quality texture, but not scaled and less accurate; as shown in Fig. 6, its resolution is way too low to guarantee a suitable readability of the signs.

To integrate the advantages of both techniques (Lastilla, 2019a), we transferred the texture from the photogrammetric model to the corresponding SLS one. This procedure is known as 'texture baking'.

Indeed, by means of the Maya software (AUTODESK, 2020a) functionality 'UV mapping' (AUTODESK, 2020b), both the UV map defined for the photogrammetric model (automatically created by Agisoft Metashape) and its texture (organized according to that UV map) were transferred to the SLS model of the Échancrée. It is worth recalling that the essential precondition for UV mapping is the perfect overlap or alignment between the two meshes.

This alignment was carried out on CloudCompare software (Girardeau-Montaut, 2019), by registering the meshes in the following way:

- Rough scaling of the photogrammetric mesh by means of a scaling factor, which was computed based on a common feature identified in both the models (see Fig. 7).
- Manual rough alignment.
- Automatic optimized alignment by means of the Iterative Closest Point algorithm (Besl and McKay, 1992), with scale adjustment enabled.

At the end of the iterative process, the RMS between the reference mesh (the SLS one) and the photogrammetric one was about 0.29 mm.

After the mesh registration was completed, the discrete distance between the point cloud of the photogrammetric model and the SLS mesh was computed, following the procedure described in Ravanelli et al. (2018). In Table 3, we report the statistics of the distance distribution; in Fig. 8, the distance distribution is shown. If we consider the distance of the photogrammetric model from the reference one as a measure of the photogrammetric model accuracy, we can notice that it is characterized, after the scale adjustment, by an RMSE of 0.31 mm (including both systematic and random errors), thus it is sufficiently accurate to guarantee an optimal texture baking.

In Fig. 9, the texture and the mesh of a portion of the model—rendered through the radiance scaling shader (Vergne et al., 2010)— are shown. In Fig. 10, the two layers are overlapped, to highlight how negligible the shift between mesh and texture is.

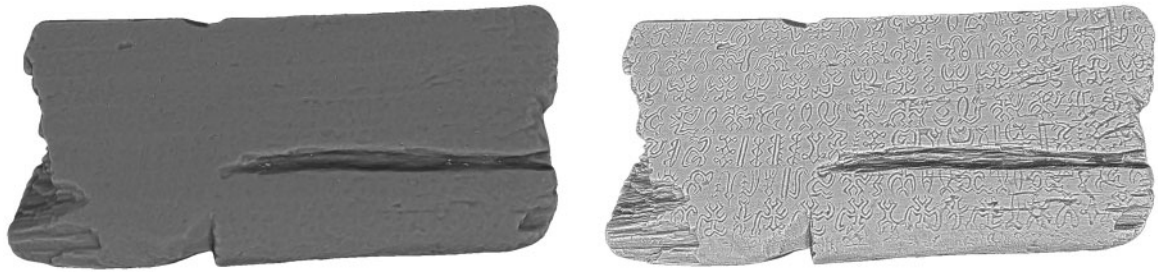

Fig. 6 Different resolutions for the photogrammetric mesh at medium quality (on the left) and the structured light scanning one (on the right), both rendered through the radiance scaling shader (Vergne et al., 2010)

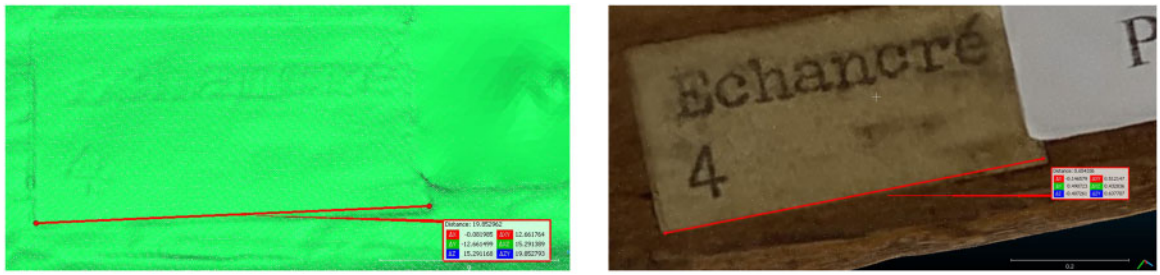

Fig. 7 Feature used to compute the scale factor between the two meshes (on the left the SLS mesh, on the right the photogrammetric model)

Table 3. Statistics of the distance distribution

Mean (mm)	Std. dev. (mm)	RMSE (mm)	Median (mm)	NMAD (mm)	Max (mm)	Min (mm)	Skewness (−)	Kurtosis (−)
−0.07	0.31	0.31	−0.09	0.23	2.40	−0.94	1.45	4.74

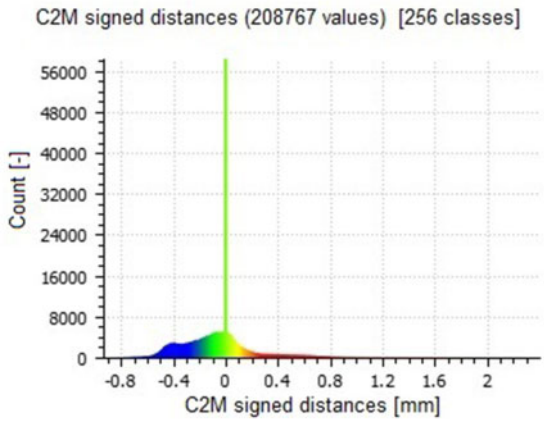

Fig. 8 Distance distribution

3.5 Final output

The final 3D model of the Échancrée tablet, obtained through integrating photogrammetry and SLS, is available on the INSCRIBE 3D Interactive Web Viewer (INSCRIBE, 2021), a WebGL 3D viewer based on 3DHOP (Potenziani et al., 2015) for basic 3D visualization (Fig. 11a) and on the Cuneiform-WebGLViewer (Fisseler et al., 2017) for enhancing the legibility of signs (Fig. 11b) by means of radiance scaling (Vergne et al., 2010).

3.6 Measurement of sign depth

One of the main advantages of 3D modelling with respect to other digitization techniques—such as Reflectance Transformation Imaging (Mudge, 2006)— is the possibility of accurately measuring sign depth. This is quite relevant from a palaeographic point of view, since it allows to disambiguate, for instance, between intentional carving and random scratches on the tablet surface. In this sense, this tablet provides an ideal specimen for this kind of application. In particular, we focused on the depth measurement for specific points (see Section 4.2).

The problem of depth measurement for the glyphs inscribed on the Échancrée tablet can be configured as an optical 3D profilometry task. This task, however, is not trivial, due to the average depth of the inscriptions (amounting to few tenths of a millimeter): indeed the error deriving from the simple assumption of perfect planarity of the tablet surface would far exceed the depth measurement, and we would lose much of the resolution provided by the 3D model. Because of this, we proceeded differently: we measured the depth of specific details at the sign scale. To this end, we set up the following procedure:

- We cropped each sign of interest from the 3D model (Fig. 12a).
- We selected some sections crossing the details of the sign (the horizontal line crossing the graphic element in Fig. 12b and the dotted curve in Fig. 13) on MeshLab (Cignoni et al., 2008).
- We obtained the cross-section average slope by linearly interpolating it (the lower dashed line in Fig. 13), to prevent our measures from being affected by this linear bias.
- We finally got the reference line for the depth measurements by translating the interpolation line up to the 'highest' point of the profile (upper continuous line in Fig. 13).
- We measured the depth of the sign (or better, of the regions of the sign crossed by the selected section) with respect to this reference line (line with oblique markers in Fig. 13).

3.7 Orthomosaic

To provide the most accurate starting point for the new transcription of the Échancrée, the orthomosaics of the two sides of the tablet were produced starting from the photogrammetric 3D model. An orthomosaic is a photogrammetrically orthorectified image generated from a set of images whose perspective distortions are corrected through a process known as orthorectification. The orthorectified images are then color balanced and merged together into a seamless orthomosaic. Indeed, distortions appear within raw images in the form of feature displacements; they are produced by factors

Fig. 9 Texture (left) and mesh (right) of the obtained model

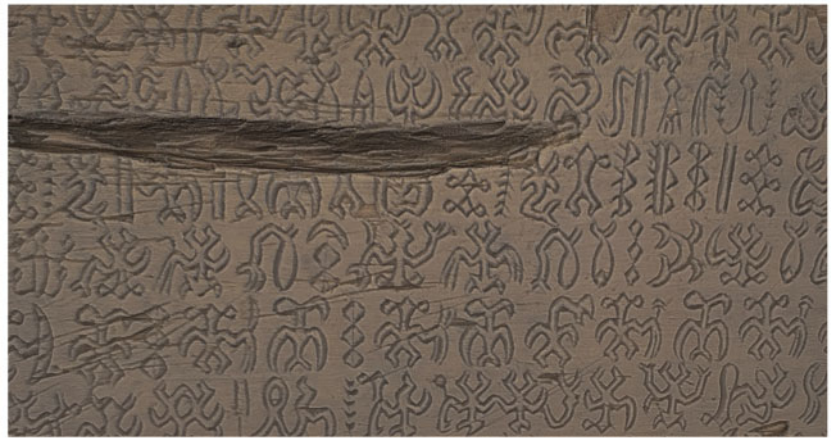

Fig. 10 Overlap between the two layers: the shift between texture and mesh is negligible

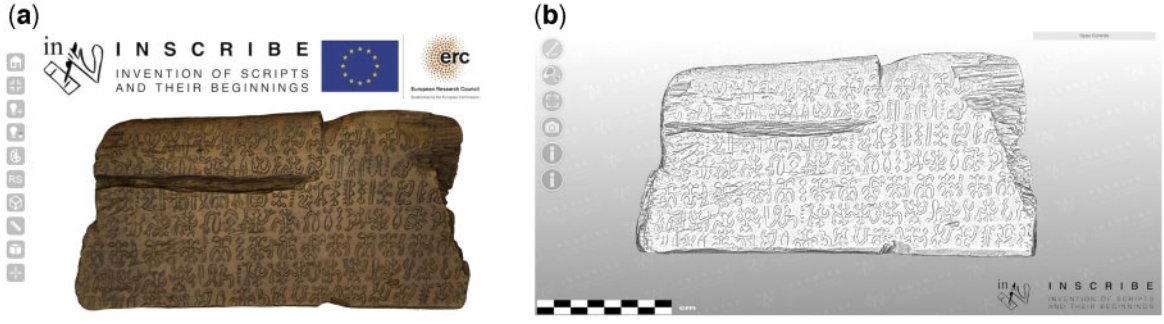

Fig. 11 The 3D model of the Échancrée tablet, comprehensive of a high quality texture and a high resolution and accurate geometry, as presented in the INSCRIBE 3D Interactive Web Viewer (INSCRIBE, 2021) with: (a) color mode powered by 3DHOP (Potenziani et al., 2015); (b) radiance scaling shading powered by the Cuneiform-WebGLViewer (Fisseler et al., 2017)

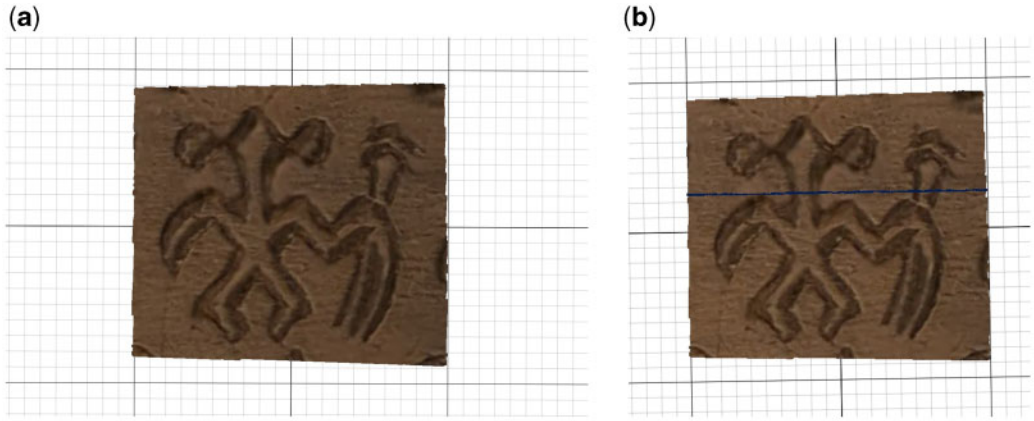

Fig. 12 Graphic element Da3.13 cropped from the 3D model (a) and an example of a cross-section selected from Da3.13, visible as a continuous horizontal line (b)

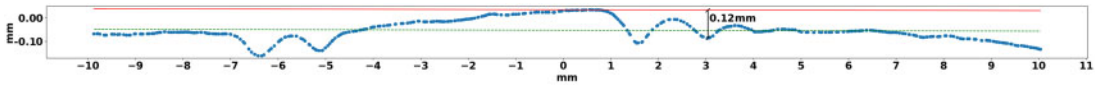

Fig. 13 Cross-section (dots), average slope of the profile (lower dashed line), reference line for depth measurements (upper continuous line) and depth measure (line with oblique markers)

such as the camera tilt, the lens distortion, and the morphology of the object surface (Baltsavias, 2006). The orthorectification process removes these perspective distortions by considering the topographical variations tied to the object's morphology, through a Digital Elevation Model (DEM is a discrete representation of the topographic surface of an object by means of a regular grid of height values), and those tied to the camera orientation, so that the errors due to elevation differences are minimized.

The result is an orthophoto, an orthogonal projection of the object's surface onto a plane; an orthophoto has therefore a constant scale wherein features are represented in their 'true' positions (OSSIM, 2021) and it can be used to measure the object in a known metric scale, exactly as in a traditional map. To compute an orthomosaic, images with a known camera orientation (interior and exterior) along with a DEM of the object surface are therefore needed. In the case of the Échancrée, the first inputs were already retrieved during the processing of the photogrammetric 3D model, whereas the DEM, together with the orthomosaic, was built once again within Agisoft Metashape.

First, the photogrammetric dense cloud was scaled using two scale bars as control and two scale bars as check, obtaining an accuracy of about half a millimeter (RMSE on check bars of 0.3 mm, RMSE on control bars of 0.5 mm). Second, for each side of the tablet, several DEMs were produced from the scaled dense cloud. In particular, Agisoft Metashape allows to project the DEM onto a plane determined by a set of markers which define the *X*- and the *Y*-axis of the plane itself. Since the two sides of the tablet are not perfectly planar and therefore there is not a unique plane which contains all the signs, seven DEMs (three for side A and four for side B, Figs. 14 and 15) were computed using different planes corresponding to diverse areas of the tablet. In this way, the residual perspective distortions were minimized by reducing, for each DEM, the areas of the tablet that are not parallel to the plane of projection.

Thus, seven orthomosaics were built with a resolution of 0.0527 mm/pix and then merged together on the basis of common features. Finally, the scale of the two overall orthomosaics was refined with a scaling factor, which was computed on the basis of a common

Fig. 14 Side A - The three areas considered for the production of the DEMs, and therefore of the orthomosaics

Fig. 15 Side B - The four areas considered for the production of the DEMs, and therefore of the orthomosaics

feature identified in each orthomosaic and the 3D model of the SLS.

4 A New State-of-the-Art for Palaeographic Analysis

4.1 A new transcription of the tablet

The digitization of the Échancrée tablet has been instrumental in creating a new drawing of the inscription (Figs. 1-2, 16–17) and thus in reassessing its palaeography. At present, the two main references for illustrations are the drawing produced by Bodo Spranz, published in Barthel (1958), and that in Fischer (1997, p. 20). These are 'normalized' representations of the inscription, in which lines are extracted from their reverse boustrophedon context and presented with the same orientation. In general, the illustrations in Barthel's work are more accurate in terms of sign shapes, but the drawing of the Échancrée is missing

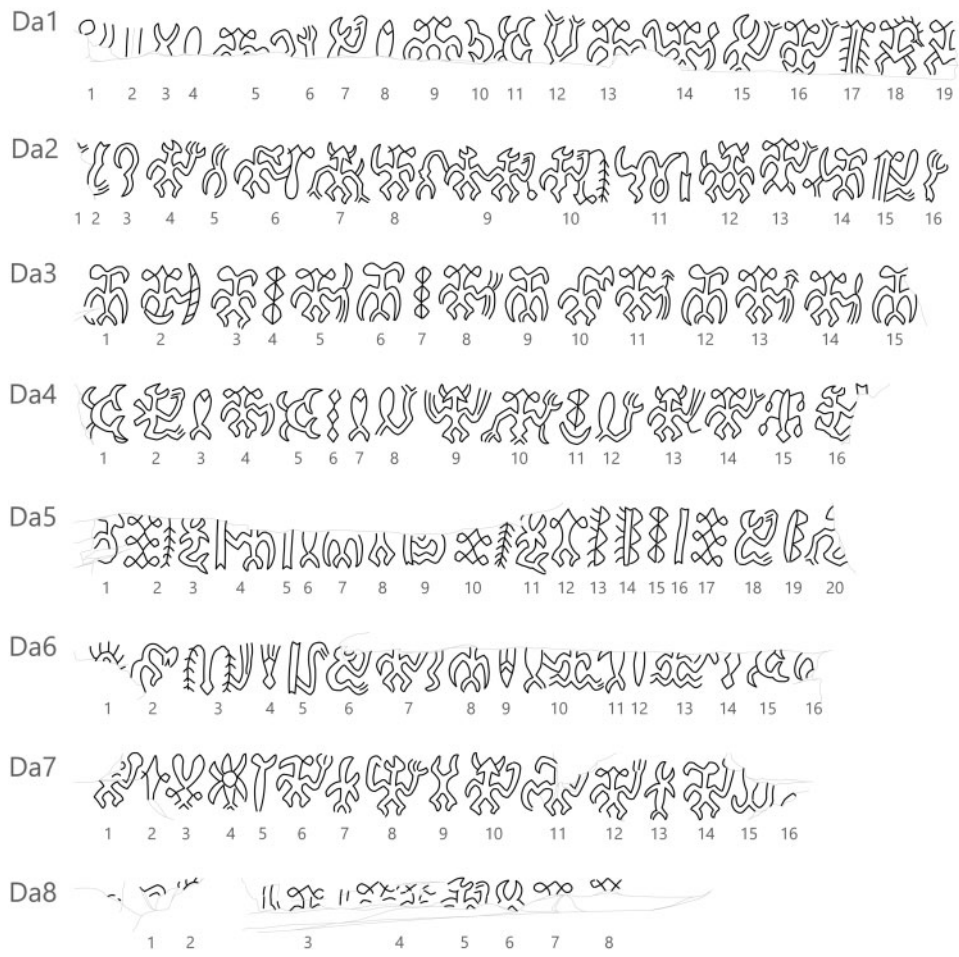

Fig. 16 Normalized drawing of the inscribed lines on side A of the Échancrée, made after the 3D model

several details, while Fischer's illustration is more complete in terms of textual content. For instance, Fischer illustrates several signs in line Da8, whereas Barthel reported the line as 'angerieben' ('rubbed off') and provided a drawing that documents only the head of one anthropomorphic glyph of the series 200.

Following is a transcription of the tablet that improves Barthel's (1958, p. 53–54) and provides a basis for palaeographic discussion. We followed Barthel's transcription system,[5] with a few exceptions that are worth specifying. Underlining represents a doubtful reading. A slash (/) separates two equally possible transcriptions: for example, Barthel's nos. 381 and 741 are probably variants of the same glyph, so we offer both as the reading of the graphic element in position Da1.7. If two alternative readings are marked with '/' and are both underlined, they are not allographs, but two different but equally uncertain possibilities. We used the symbol • to mark uncertainty about (1) one glyph or (2) one part of an anthropo- or theriomorphic glyph in the 200–700 series, in which (following Barthel's system) each of the three digits tends to reflect a different body part or attachment. Thus, '68•' means that the glyph is one of the five in the 680 series of the catalogue, which represent a two-headed bird with a long beak, but we cannot determine which because its lower portion is not preserved.

Fig. 17. Normalized drawing of the inscribed lines on side B of the Échancrée, made after the 3D model

4.1.1 Side *A*

Da1

]•–•–•–•–2•1(−)6–381/741–700–208–7y–7–94–207–63.207s–734–204–5f–522f–99[

Da2

]•–60–78/79–306y–56–460.90–590V.s–205–75.300y.301s–441.95x.3–445.107.1–s594–284–s605–173(=5.225/325)–6–[

Da3

] 600–42:200.41/11–610–2–200.52x.s–600–2–200.52x.52–600–460–200.52x.69–600–200.52x.69–200.52x.s–600[

Da4

]7–371/379(.61)–700–207–7–2V–700–73.64–52x.590.52x–(6x.)206s–42:2–73.6–590.52.s–204–34–370.1[

Da5

]380y–2V.3–730–1.400/600–1–700–400/600–93–1.380y–2V.3–730–93–20cfy–20bfy(=1f.20y?)–2–1–2V–381/741–20dy–37•[

Da6

]59–470–3.3.52–50–1.6/61–38•–20•/30•.78/79–400/600–50–700.240/340–700–•–243–•–7–60•[

Da7

]202–95–94a/116–81–450–526–739–301y.6–83–590.61–607–206–739–605–•[

Da8

]•–• [. . .]–2••–2••.2••–3•6–84–•(−)•[

4.1.2 Side *B*

Db1

]246/256–1–200.52–371/731–371/731–306.56/74(−)41–3•2–464.•–2–68•–464.•–2–3••/40•–•[

Db2

]590.56–25.10–9.6.3–606s.3–82.6.3–667/670.3–93f.93f–606s–73.6–8–59.6–520f–•••[

Db3

]383–383–13.6.74–1.63–1.63–7.3–4.6–4.94a/116–2–2–280.63–12–93–200–•••[

Db4

]1–381/741–630–50–50–1–700.244–700.244–240.8–240.8–22–7–600–7.10–•[

Db5
]522f.700–2.9–200.524f.78–6–700:6–622–381/741–1–8–40V–8–69.108/109–445–445[
Db6
]244/254–55–9–44/79–608V/633–6/55–7–600–7–68•–s234–93f–42:9–22f[

Given the damaged condition of some parts of the tablet, especially the edges, and the 'deep gash' on side A, several glyphs are severed, and it is hard to determine whether they were written jointly or not. Moreover, it remains difficult to establish what a 'basic sign' or grapheme in the Rongorongo script was. Thus, we opted for counting the number of 'graphic elements' preserved on the Échancrée. *Graphischen Elemente* is a term originally used by Barthel (1958, p. 12, and *passim*) to refer to his individualized characters. Yet while ligatures of two or more sign shapes could in theory function as independent Rongorongo signs, with their own specific reading, Barthel still treated some of them as mere additions of smaller units. Damage to the tablet and our ignorance of the mechanics of the script make a precise count difficult. To avoid assumptions, we followed a criterion different from Barthel's. Thus, each graphic element we counted is just a cohesive unit formed by one self-standing glyph or the apparent junction of multiple shapes. A conservative count following this criterion indicates that the tablet features 212 graphic units.

4.2 Notes on palaeography

In the following section, Da 1.1 refers to the first graphic element in the first line of side A, and so forth.

4.2.1 Da1.18-19

For Barthel (1958, p. 53), the last two elements of the inscription were 522f–522. Indeed, what is preserved of the last element does not show multiple strokes (Barthel's f-feature) on its head. This is noteworthy because, apart from 526 in Da7, the other glyphs of the 520 series (anthropomorph with adorned headdress?) found in the tablet are drawn with these optional strokes (Db2.12 and Db5.1, 3). Thus, the last element in the line could be 99, which is similar to 522 in its lower half but features a frontal head instead. Moreover, while there is no other instance of 522–522 in the Rongorongo corpus, the sequence 522–99 is attested in Tablet R ('Small Washington').[6] In fact, the 204–5f–522f–99[at the end of Da1 is reminiscent of 206s–522f–99 in Rb2.

4.2.2 Da2.11

Here, we find a unique ligature with three components, which Barthel left untranscribed. Starting from the left, the first component is consistent with the anthropomorphic glyph catalogued as no. 445 by Barthel, but lacks the head. Glyph 445 appears elsewhere in the Échancrée (Db5.13, 14) and is similar to glyph 441, which is part of the immediately preceding element 441.95x.3 (Da2.10). The loss of the head (possibly not its most meaningful part in terms of iconicity) seems due to its attachment to the second component, a holed or looped shape that finds its best match in Barthel's no. 107. The third component is the bar-looking glyph no. 1, which Fischer illustrated as united with a discontinuous line. Yet, our 3D model confirms that the attaching line depicted in Barthel (1958) is clearly incised (Figs. 18 and 19). The reduction of glyph 1 is common in the corpus (see Aa8, Ab4, Bv9, Ca1, Ca2, Ca3, Ca5, Ev3, Gr3 = Kr3, Hr8 = Pr7 = Qr7, Ra6, Rb1, Sa1), but elsewhere it is not attached to the preceding graphic element through a line. The phenomenon is mainly involved in two repeating Rongorongo sequences: variations of 67(.SIGN) (.) 460/470/490–1 as part of a longer sequence in Ab4, Ev3, Gr3, Kr3, Ra6, and Sa1, in which it alternates with the normal-sized version of itself (see Cb2); and (22.)243–1 (22) in Aa8, Ca3, Hr8, Pr7, and Qr7. However, we also find a reduced 1 in the sequence 455–1, in Ca1, which is reminiscent of our ligature. In comparative perspective, this use of the attaching line in the Échancrée supports the idea that whenever 1 is reduced, it forms a meaningful unit with the preceding graphic element.

4.2.3 Da2.15

Ligatured glyph 173 is found only on this inscription. It is a conflation of glyph 5 (on the left) and part of an anthropomorphic glyph (on the right), either 225 (human with frontal face with outstretched leg and raised limb) or 325 (the same but with head in profile). The part employed in this ligature comprises only the upwards arm and the leg (represented by the digits -25). 173 is therefore comparable to ligature 5.325, comprising the complete anthropomorphic glyph, as attested in line Ab1 of Text A or *Tahua*.

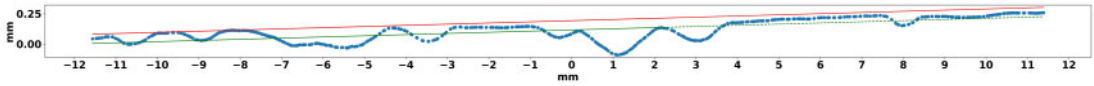

Fig. 18 Horizontal section of Da2.11. The dotted blue curve represents the surface of the tablet. It indicates that the line attaching shape no. 1 to the Rongorongo ligature (eight and last depression on the right) is as deep as the incisions of the raised limb of shape no. 445 (the first two depressions on the left)

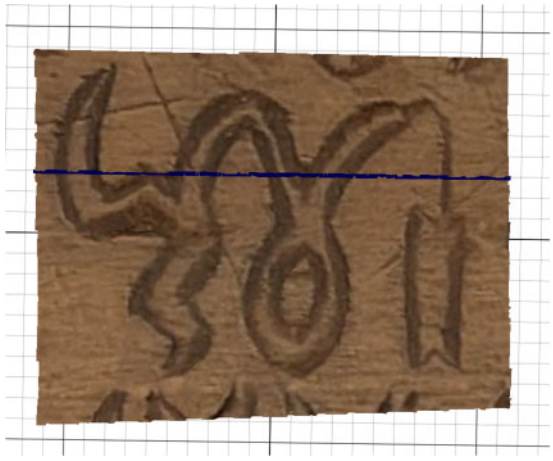

Fig. 19 Cross-section of Fig. 18 shown as a continuous horizontal line on the crop of the graphic element Da2.11

Such processes of conflation are already well documented for Rongorongo (see e.g. the reduction of (200.)25.226/326 > 171 in Horley, 2007, p. 30, Fig. 5) and are crucial to make progress in understanding the mechanics of the script.

4.2.4 Da3.2

The rightmost component of 42:200.41/11 is crossed by scratches to the tablet, but there are at least four oblique lines inside of it that seem like intentional carving (Fig. 16). Their depth (between 0.48 and 0.32 mm) is greater than most scratches and comparable to the depth of other signs. Moreover, two other Rongorongo inscriptions also feature what is seemingly crescent-shaped glyph no. 41 with inner crossing strokes: two instances in Text B (83.41 in Br9 and 41.8 in Bv10) and one in Text S (41 in Sb6). What remains uncertain is whether these intentional strokes reflect a mistaken no. 41 that was corrected to no. 11 (vertical bar with crossing inner strokes), in what would then constitute a common mistake, or rather a variant of glyph 41 with an unknown function.

4.2.5 Da5.8

This broken element can only match glyphs 93, 511, 571, or 591. Three facts combined suggest that 93 is the most probable: (i) the inscription follows an iterative pattern and this is also the case with line Da5, whose first eight graphic elements (]380y–2V.3–730–1.400/600–1–700–400/600–?) are echoed by the following 1.380y–2V.3–730–93 (with 93 occurring in position Da5.12) and (ii) out of the four possible glyphs mentioned above, 93 is the only one that is attested in the inscription: in addition to Da5.12, it occurs twice on side Db.

4.2.6 Da6.3-4

The element in position Da6.3 is a ligature of at least two separate shapes. The shape on the right is Barthel's net-like glyph no. 52 in its upwards version; the shape on the left is more difficult to interpret. It was treated by Barthel as comprising in turn three shapes, namely two glyphs no. 3 (hanging cord, plant, or ornament?), attached to the left and to the right of an unidentified looping shape. This ligature is also found in Tablet C (*Mamari*), in line Cb11, which Barthel again represented as a ligature with the structure 3.SIGN.3, and possibly in Tablet G ('Small Santiago'), in line Gv1, as part of a larger compound identified as 3.95x.3.76. Barthel's transcription of the mid-bottom part of the latter as a vertically inverted glyph 95 is due to its looping aspect, identical to the frontal head 95. However, this twisting feature, with side loops that are optional, characterizes not only certain anthropomorphic glyphs, but also glyphs of other kinds. It is not necessarily no. 95. One possibility is that the whole ligature is rather an upside-down variant of glyph 30 (which probably depicts twisted or looping cordage). Another possibility, more likely, is that it is simply the union of two glyphs no. 3. Due to its characteristic dangling shape, 3 is always attached to the preceding or following shape (Davletshin, 2012, p. 247). Thus, the pointed (and optionally looping) feature may be a

graphic device for uniting two instances of a glyph that, by definition, was never carved self-standing.

The variant of glyph 50 in Da6.4, though similar to other attestations (see texts Cb13, Hr4, Hr8, Hv5, Hv10, Pr4, Pv7, Sa6, and Sb7-8), is not common. It lacks the double inverted-V feature at mid-height and its lower tip is quite distinct from the other instance of the sign in the same line (Da6.9). Probably it began to be incised, by mistake, like the left-part shape of the preceding ligature, 3.3.52. Their lower portions are identical, both being shaped like a lozenge. Afterwards, it would have been corrected, but only the top part acquired the broom-like shape that characterizes it.

4.2.7 Db3.11

This is a ligature, most likely of Barthel's glyphs no. 280 (often called 'Turtle' in the literature) and 63 (axe or adze). The head of the creature is damaged, but appears to be split, as illustrated in Fischer's drawing. The upper limbs are drawn in a continuous manner, so that the lines cross the carapace. This variant is attested only five times for shape 280, twice in Aa8, twice in Pv7, and once in Pv9.

4.2.8 Db6.2, 6

These hand glyphs seem to be zigzagging, especially the first one, which also has traces of looping corners. These characteristics point to instances of glyph 55, rather than 6, as implied by Barthel and Fisher's editions. Moreover, 55 seems to be detached from 9 in Db6.2-3.

4.2.9 Db6.14

There seem to be preserved intentional strokes (at least two, but possibly four) on the right part of the glyph, which allow us to suggest reading this element as 22f, rather than 41.

4.3 Analysis of parallel passages and possible textual content

Several Rongorongo tablets either contain the same text (this is the case of G and K, and H, P and Q), or share many fragments of text (Horley, 2007, is the most recent detailed account). However, Horley (2007, p. 26, Fig. 1) reports that only line Da3 and part of line Db2 contain 'structured sequences or repetitive patterns', with the rest of its textual contents being independent. Our analysis confirms that the inscription on the Échancrée is largely different from the remaining Rongorongo texts. If considered together, the sequences •–7–60• [(Da6.14–16), 7–600–7.10–• [(Db4.12–15), and 7–600–7 (Db6.7–9) remind us of 66–7–600–7.10, found twice in line Sb6 of Tablet S or Large Washington (for the latter, see Horley, 2013, p. 51). However, only 7–600–7.10 is an exact match. Similarly, 445.107.1–s594–284 (Da2) is reminiscent of 386–65.1–594–206s–22 (Hr10) = 381–65.1–594–200.22 (Pr9). Yet, with this we exhaust the most obvious parallels between glyph groups of the Échancrée and other Rongorongo texts. This lack of shared contents is unlikely to be an accident induced by the small size of the text. Other short inscriptions, such as K and N (both comprising approximately 170 graphic elements according to our count), have extensive contents in common with other Rongorongo inscriptions.

Conversely, the text of the Échancrée has a series of iterative elements or sequences of elements on both sides, more than what has been reported before. In line Da3, the strings 610–2–200.52x.s, 600–2–200.52x.52, 600–460–200.52x.69, and 600–200.52x.69–200.52x.s seem like repetitions of the pattern bird-sign 600 (or 610) + changing glyph + 205.52x.appendage.[7] In line Da4, the successive 2V–700–73.64–52x.590.52x–(6x.)206 and 42:2–73.6–590.52.s–204 appear to be variations of the same sequence, especially if we bear in mind that raised hand glyphs 64 (also part of 204) and 6 (also part of 206) behave like allographs (Pozdniakov, 1996, p. 295). In Da5,]380y–2V.3–730 and 1.380y–2V.3–730 are identical, and it is possible that the broken element at the beginning of the line was originally [1.]380y. Most of the inferior half of line Db1 is lost, but there seems to be a repetition of 464.•–2. In line Db2, four consecutive elements are ligatures with glyph 3 attached on the right. Db3 contains duplications of graphic units:]383–383, 1.63–1.63, and 2–2. Db4 does the same with 50–50, 700.244–700.244, and 240.8–240.8. Db5 repeats 445 at the end of the line.

Thus, the text of the Échancrée is comparable to the majority of the better-preserved Rongorongo tablets in featuring 'structured sequences' (see e.g. Guy, 1982; Horley, 2007, p. 25), even though it lacks repeated glyphs functioning as 'entry markers' or 'delimiters' and forming 'list-like' structures, as seen in several

tablets (especially A, C, E, G, K, H, N, P, and Q). This means that while the precise textual content of the Échancrée may be different, structurally it is of a type similar to other inscriptions.

Interpreting what kind of text may underlie the inscription is of course a problem tied to the undeciphered status of Rongorongo and is hindered by our ignorance of what constituted a sign (a graphemic unit with a single value) and what a sign represented. Rongorongo probably represents a script *stricto sensu*, as suggested above, with phonograms (signs standing for speech sounds) as well as at least some logograms (signs standing for words) (see e.g. Pozdniakov, 1996; Horley, 2007; Davletshin, 2012, 2016). However, the existence of semantic determinatives or 'taxograms' (Guy, 2006, Horley, 2007, p. 26), i.e. signs which are not read and just indicate the semantic sphere of words spelled, is still debated.

Also disputed is the type of phonetic signs the script may have possessed: most scholars (Macri, 1996; Horley, 2007; Pozdniakov and Pozdniakov, 2007; Davletshin, 2012) think that phonetic signs are most likely syllabic, but Guy (1990, p. 141–145, 2006) has suggested a few compelling readings in a calendrical text of Tablet C that would point to the existence of two-syllable phonograms. In any case, iterations of identical or similar sequences, of two or three graphic units, could stand for Rapanui words (perhaps even words comprising duplicated morphemes of the type of e.g. *mangamanga* 'finger') or short sentences. Thus, the text would take the form of a series of related lexical items or phrases. This is not inconsistent with the tentative interpretations of subject-matters inferred by scholars, including certain kinds of charms, recitations, or songs (Pozdniakov, 1996, p. 299; Horley, 2007, p. 30). Conversely, the lack of graphic elements whose distribution mirrors that of common grammatical words in spoken Rapanui (e.g. the article *te*, or the prepositions *ki* 'to' and *i* 'in, at') makes it improbable that what we have here represented is a complex form of prose.

5 Concluding Remarks

Any palaeographic analysis needs to include all known specimens of this script. Until that goal is reached, all examination and reassessment is limited and piecemeal. This contribution aims to add in that direction, with a complete palaeographic analysis of the Échancrée tablet, a new transcription, a state-of-the-art 3D model, and a search for features paralleled in other texts. The research around other Rongorongo inscriptions is ongoing and it is expected that their continuous study will shed unprecedented light on this mysterious script.

The pursuit of a definitive decipherment, due to the paucity of the corpus, cannot rely on any less than an accurate transcription of each text. Achieving a new state-of-the-art geared towards that end implies that advanced technologies must be applied and integrated to a traditional study of the palaeography of the inscriptions. Accurate text analysis, in other words, hinges directly on accurate 3D models of the tablets, and corrections of previous hand drawings and transcriptions, to reach unbiased 'readings'. Ultimately, the new modelling of the Échancrée tablet has made all of this possible for the first time.

Funding

This research is part of the ERC Project "INSCRIBE. Invention of Scripts and Their Beginnings" (awarded to SF). The project has received funding from the European Research Council (ERC) under the European Union's Horizon 2020 research and innovation program (Grant Agreement No. 771127).

Notes

1. See the updated list of inscriptions currently accepted as authentic in Horley and Pozdniakov (2018, p. 82) and Horley et al. (2018, p. 336–338).
2. These are the most widely used labels. Thomson (1891, p. 42–43) labelled the tablet *Ka Ihi Uiga*. These are the three first words of a chant sung by the native Ure Va'e Iko, to whom Thomson showed a photograph of one of the inscriptions in Bishop Jaussen's possession at that time, in the hopes that he would assist their decipherment (*ibid.*: 525). Fischer (1997, p. 419) catalogued it as RR 3, following his alphanumerical system.
3. The tablet dimensions were measured based on the 3D model bounding box, having previously adjusted it by means of principal component analysis (PCA).

4. See also Horley (2013 p. 38–39) and Horley et al. (2018, p. 333–334). In the latter work, it is argued that tablet S was re-shaped to be recycled as a canoe plank (losing ca. 0.5 cm of its original height), which makes it likely that originally it was even more similar to P.
5. A short note on the epigraphic apparatus is in order. Following Barthel (1958, p. 41), a, b, c, d, e = specific palaeographic variants of a glyph; f = shape is provided with multiple additional strokes around its contour; s = Barthel's so-called *Schmuckelement* ('decorative element') whose function remains uncertain but may not be merely ornamental; x = shape vertically inverted; y = shape horizontally inverted. We use 'V' in a more general way than Barthel to indicate that this is a specific variant of a glyph (in some cases, we may be dealing with a different sign). A small dot represents the joint writing of two shapes on a horizontal axis and a colon (:) stands for vertical ligaturing.
6. Notice, however, the similar string 523f–522f in Cb5 (whose reading we will reassess elsewhere). We thank one of the anonymous reviewers for referring us to this instance.
7. This pattern was already recognized by Fischer (1997, p. 423) as 'an accretive suffixal series attached to the hand of each anthropomorph'. However, the author tentatively speculated about a 'potential numerical series', whereby each 'suffix' would represent a Rapanui numeral ('*e tahi* 'one', '*e rua* 'two', and so forth).

Acknowledgements

The authors are very grateful to the Congregation of the Sacred Hearts of Jesus and Mary, Rome, where the inscriptions are housed, for their kind assistance during repeated visits, in particular to Father Alberto Toutin Cataldo, Father Éric Hernout, and Mrs Luana Tarsi. They are also thankful to Paul Horley, for the discussion on matters related to the documentation of epigraphical features, and to Rafał Wieczorek, for pointing us to bibliographical references. Finally, they wish to thank the anonymous reviewers for their valuable insight.

Conflicts of Interest

The authors declare no conflict of interest.

References

Affatato, S., Valigi, M., and Logozzo, S. (2017). Wear distribution detection of knee joint prostheses by means of 3D optical scanners. *Materials*, **10**(4): 364.

Agisoft Metashape. (2020a). Agisoft Metashape. https://www.agisoft.com/ (accessed October 2020).

Agisoft Metashape. (2020b). How to build a complete (360 degree) model of an object. https://agisoft.freshdesk.com/support/solutions/articles/31000155265-how-to-build-a-complete-360-degree-model-of-an-object (accessed October 2020).

AUTODESK. (2020a). Maya. https://www.autodesk.it/products/maya/overview (accessed October 2020).

AUTODESK. (2020b). UVs. https://knowledge.autodesk.com/support/maya/learn-explore/caas/CloudHelp/cloudhelp/2020/ENU/Maya-Modeling/files/GUID-FDCD0C68-2496-4405-A785-3AA93E9A3B25-htm.html (accessed October 2020).

Baltsavias, E., Zhang, L., Holland, D., Srivastava, P. K., Gopala Krishna, B., and Srinivasan, T. P. (2006). Extraction of geospatial information from high spatial resolution optical satellite sensors. In: *ISPRS Technical Commission IV Symposium "Geospatial Databases for Sustainable Development"*. https://www.isprs.org/education/pdf/GOA_BGK_Orthoimage_Section5.pdf.

Barthel, T. (1958). *Grundlagen zur Entzifferung der Osterinselschrift*. Hamburg: Walter de Gruyter.

Besl, P. J. and McKay, N. D. (1992). Method for registration of 3-D shapes. Sensor fusion IV: control paradigms and data structures. *International Society for Optics and Photonics*, **1611**: 239–56.

Carrero-Pazos, M. and Espinosa-Espinosa, D. (2018). Tailoring 3D modelling techniques for epigraphic texts restitution. Case studies in deteriorated roman inscriptions. *Digital Applications in Archaeology and Cultural Heritage*, **10**: e00079.

Cignoni, P., Callieri, M., Corsini, M., Dellepiane, M., Ganovelli, F., and Ranzuglia, G. (2008). Meshlab: an open-source mesh processing tool. *Eurographics Italian Chapter Conference*, **2008**: 129–36.

D'Aranno, P. J. V., De Donno, G., Marsella, M., et al. (2016). High-resolution geomatic and geophysical techniques integrated with chemical analyses for the characterization of a Roman wall. *Journal of Cultural Heritage*, **17**: 141–50.

Davletshin, A. (2012). Numerals and phonetic complements in the *Kohau Rongorongo* script of Easter Island. *Journal of the Polynesian Society*, **121**(3): 243–74.

Davletshin, A. (2016). Word-signs and sign groups in the Kohau Rongorongo script of Easter Island. In Conrich, I. and Mueckler, H. (eds), *Easter Island: Cultural and Historical Perspectives*. Berlin: Frank & Timme, pp. 201–16.

Esen-Baur, H.-M. and Santos, P. (2019). Digitization project of all extant Rongorongo tablets. In Vogt, B., Kühlem, A., Mieth, A. and Bork, H.-R. (eds), *Proceedings of the 9th International Conference on Easter Island and the Pacific*, held in the Ethnological Museum Berlin, Germany, from June 21–26, 2015. Easter Island: German Archaeological Institute/Rapanui Press, pp. 385–92.

Fischer, S. R. (1997). *Rongorongo: the Easter Island Script: History, Traditions, Texts*. England: Clarendon Press.

Fisseler, D., Müller, G. G. and Weichert, F. (2017). Web-based scientific exploration and analysis of 3D scanned cuneiform datasets for Collaborative Research. *Informatics*, **4**(4): 44.

Francolini, C., Marchesi, G. and Bitelli, G. (2018). High-resolution 3D survey and visualization of Mesopotamian artefacts bearing cuneiform inscriptions, vol. 2018. 2018 Metrology for Archaeology and Cultural Heritage (MetroArchaeo), Cassino, Italy, pp. 183–187.

Girardeau-Montaut, D. (2019). Cloud compare—3D point cloud and mesh processing software. Version 2.10.2. https://www.danielgm.net/cc/ (accessed October 2019).

Guy, J. B. M. (1982). Fused glyphs in the Easter Island script. *Journal of the Polynesian Society*, **91**: 445–447.

Guy, J. B. M. (1990). The lunar calendar of Tablet Mamari. *Journal de la Société des Océanistes*, **91**: 135–149.

Guy, J. B. M. (2006). General properties of the Rongorongo writing. *Rapa Nui Journal*, **20**: 53–66.

Horley, P. (2007). Structural analysis of Rongorongo inscriptions. *Rapa Nui Journal*, **21**(1): 25–32.

Horley, P. (2009). *Rongorongo* script: carving techniques and scribal corrections. *Journal de la Société des Océanistes*, **129**: 249–261.

Horley, P. (2011). Palaeographic analysis of the Santiago Staff. *Rapa Nui Journal*, **25**(1): 31–43.

Horley, P. (2012). *Rongorongo* tablet from the Ethnological Museum, Berlin. *Journal de la Société des Océanistes*, **135**: 243–256.

Horley, P. (2013). The large *rongorongo* tablet from the collections of the Smithsonian Institution, Washington, D.C. *Rapa Nui Journal*, **27**(1): 37–61.

Horley, P. and Pozdniakov, K. (2018). L'écriture de l'île de Pâques. In Pierre, A., Blanquer-Maumont, A., and Ramio, C. (eds), *L'île de Pâques. Actes Sud/Musée Champollion—Les écritures du monde*, Figeac/Musée Fenaille, Rodez/Muséum d'Histoire Naturelle de Toulouse, pp. 80–93.

Horley, P., Davletshin, A., and Wieczorek, R. (2018). Rongo-Rongo: How many scripts were there on Easter Island? In Jakubowska-Vorbrich, Z. (ed.), *The Sleep of Reason Produces Monsters: Misconceptions about Easter Island in Light of 21st Century Science*. Warsaw: Museum of the History of the Polish Popular Movement, pp. 323–468.

INSCRIBE. (2021). *INSCRIBE 3D Interactive Web Viewer*. https://www.inscribercproject.com/3d_viewer_home.php (accessed April 2021).

Lastilla, L., Ravanelli, R., and Ferrara, S. (2019a). 3D high quality modeling of small and complex archaeological inscribed objects: relevant issues and proposed methodology. *The International Archives of the Photogrammetry, Remote Sensing and Spatial Information Sciences*, **XLII-2/W11**: 699–706.

Lastilla, L., Ravanelli, R., Valério, M., and Ferrara, S. (2019b). 3D modelling of the Mamari tablet from the Rongorongo corpus: Acquisition, processing issues and outcomes. *The International Archives of the Photogrammetry, Remote Sensing and Spatial Information Sciences*, **XLII-2/W18:** 85–9.

Macri, M. J. (1996). Rongorongo of Easter Island. In Daniels, P. T. and Bright, W. (eds), *The World's Writing Systems*. Cambridge: Cambridge University Press, pp. 183–8.

Mudge, M., Malzbender, T., Schroer, C., and Lum, M. (2006). New reflection transformation imaging methods for rock art and multipleviewpoint display. In Ioannides, M., Arnold, D., Niccolucci, F., and Mania, K. (eds), *The 7th International Symposium on Virtual Reality, Archaeology and Cultural Heritage*. Nicosia, Cyprus: VAST.

Orliac, C. (2007). Botanical identification of the wood of the large kohau Rongorongo tablet of St. Petersburg. *Rapa Nui Journal*, **21**(2): 7–10.

Orliac, C. (2010). Botanical identification of 200 Easter Island wood carvings. In: Wallin, P. and Martinsson-Wallin, H. (eds), *The Gotland Papers: Selected Papers from the VII International Conference on Easter Island and the Pacific*. Visby: Gotland University Press, pp. 125–139.

OSSIM. (2021). *Orthorectification*. https://trac.osgeo.org/ossim/wiki/orthorectification (accessed January 2021).

Potenziani, M., Callieri, M., Dellepiane, M., Corsini, M., Ponchio, F. and Scopigno, R. (2015). 3DHOP: 3D heritage online presenter. *Computers & Graphics*, **52**: 129–141.

Pozdniakov, K. (1996). Les bases du déchiffrement de l'écriture de l'île de Pâques. *Journal de la Société des Océanistes*, **103**(2): 289–303.

Pozdniakov, K. (2011). Tablet Keiti and calendar-like structures in Rapanui script. *Journal de Société des Océanistes*, **132**: 39–74.

Pozdniakov, I. and Pozdniakov, K. (2007). Rapanui writing and the Rapanui language: preliminary results of a statistical analysis. *Forum for Anthropology and Culture*, **3**: 3–36.

Ravanelli, R., Lastilla, L., Nascetti, A., et al. (2018). 3D modelling of archaeological small finds by the structure sensor range camera: comparison of different scanning applications. *Applied Geomatics*, **10**(4): 399–413.

Remondino, F., Guarnieri, A. and Vettore, A. (2005). 3D modeling of close-range objects: photogrammetry or laser scanning? *International Society for Optics and Photonics*, **5665**: 56650M.

Spring, A. P. and Caradoc P. (2014). Developing a low cost 3D imaging solution for inscribed stone surface analysis. *Journal of Archaeological Sciences*, **52**: 97–107.

Thomson, W. J. (1891). Te Pito te Henua, or Easter Island. Report of the National Museum of Natural History for the Year Ending June **30, 1889**. In *Annual Reports of the Smithsonian Institution for 1889*. Washington, DC: Smithsonian Institution, pp. 447–552. https://tinyurl.com/cjsc8w5d.

Valente, R. and Barazzetti, L. (2020). Methods for ancient wall graffiti documentation: overview and applications. *Journal of Archaeological Science: Reports*, **34**.

Vergne, R., Pacanowski, R., Barla, P., Granier, X., and Schlick, C. (2010). Radiance scaling for versatile surface enhancement. In *Proceedings of the 2010 ACM SIGGRAPH Symposium on Interactive 3D Graphics and Games*, ACM, pp. 143–50.